In silico molecular docking evaluation reveals high potencies of some natural antifungal metabolites on melanin biosynthesis and appressoria formation enzymes in Magnaporthe oryzae

Md. Arif Khan
University of Development Alternative
Md. Abdullah Al Mamun Khan
Mawlana Bhashani Science and Technology University
Jannatul Maowa Sanjana
Mawlana Bhashani Science and Technology University
Asif Ahsan
Bangladesh Agricultural University
Dipali Rani Gupta
Bangabandhu Sheikh Mujibur Rahman Agricultural University
M. Nazmul Hoque
Bangabandhu Sheikh Mujibur Rahman Agricultural University
Tofazzal Islam (tofazzalislam@yahoo.com)
Bangabandhu Sheikh Mujibur Rahman Agricultural University

Article

Keywords: Molecular docking, Antifungal metabolites, Melanin biosysthesis, Magnaporthe oryzae

Posted Date: June 29th, 2022

DOI: https://doi.org/10.21203/rs.3.rs-1794320/v1

Abstract

Magnaporthe oryzae is one of the most notorious fungal pathogens that causes blast disease in cereals and results in enormous loss of grain production. Many chemical fungicides are being used to control the pathogen but none of them are effective against blast disease. Thus, there is a demand to discover potential and safe natural biofungicides to manage blast disease successfully. To find out effective biofungicides, we performed in silico molecular docking analysis of some natural compounds targeting four enzymes namely, scytalone dehydratase, SDH1 (1STD), trihydroxynaphthalene reductase, 3HNR (YBV1), trehalose-6-phosphate synthase, Tps1 (6JBI) and isocitrate lyase, ICL1 (5E9G) of M. oryzae fungus that regulate melanin biosynthesis or appresorium formation. Thirty-nine natural compounds that previously reported to inhibit the growth of M. oryzae were subjected to rigid and flexible molecular docking against aforementioned enzymes followed by molecular dynamics simulation and free energy analysis of protein-ligand complexes. The results of virtual screening showed that out of 39, 12 compounds showed good binding energy with any one of the target enzymes as compared to reference molecule azoxystrobin and strobilurin. Among the compounds, camptothecin GKK1032A2 and arohynapene-B bind more than one target enzymes of M. oryzae. All the compounds except tricyclazole showed good bioactivity score. Taken together, our results suggest that all of the 12 compounds have the potential to develop new fungicides but camptothecin, GKK1032A2 and arohynapene could act as multi-site mode of action fungicides against M. oryzae.

1. Introduction

Blast disease caused by the *Magnaporthe oryzae* (anamorph: *Pyricularia oryzae*), is one of the most destructive diseases of cereals including rice, wheat, barley, finger millet etc. [1,2]. Approximately 10–30% of the global rice production is lost by the infections caused by this recalcitrant pathogen [3]. Although rice blast is prevalent in most rice-growing regions in the world wheat blast was confined only to South American countries, including Brazil, Bolivia, Argentina, and Paraguay until 2015 [4]. The disease was first time reported in an Asian country, Bangladesh, in February 2016 [5]. Some newspaper in India has also reported the existence of the disease in border districts of India that are close to wheat blast infected districts of Bangladesh [6]. Very recently, this disease has also been reported in the Gambia, an African country, apart from South America and Asia [7]. Air-borne inoculum is the mechanism of short-distance disease spread whereas, seed trading is thought to be the mechanism of disease spread over a long distance [4,8]. Although the rate of devastation by the disease depends on several factors but can cause yield loss of up to 100% in a congenial environment [2,9].

The genus of *M. oryzae* consists of several pathotypes and can cause blast disease on more than 50 Poaceae plants [10]. Based on host specificity they are classified as *Oryza* pathotype (infecting rice), *Triticum* pathotype (infecting wheat), *Setaria* pathotype ((infecting foxtail millet), *Lolium* pathotype ((infecting ryegrass), and many other [11,12]. Although the isolates from different hosts are genetically distinct, cross-infection does occur to some extent [4,13]. As *M. oryzae* isolate of wheat can infect barley, maize triticale, durum and swam rice grass in laboratory conditions whereas *M. oryzae* isolates of rice can cause disease in the wheat plant [5,14,15]. However, the virulence of these pathogens during cross-infection in field conditions has not been tested yet.

The control of blast disease is difficult and mainly achieved through the use of chemical fungicides [16,17]. However, extensive use of chemical fungicides has led to acquired resistance against fungicides [2,17]. Moreover, traditional breeding strategies take a longer time to develop resistant variety and resistance often breakdown in field conditions after certain years due to quick evolution of the pathogen [10,18]. Therefore, development of new fungicides by searching for bioactive natural compounds is a novel approach to managing destructive diseases. Various research studies have been carried out to estimate the antifungal potential of natural compound against blast fungus *in vitro* however, filed efficacy of these compounds are still unclear [19–21]. Most of the natural compounds act directly on fungal cell whereas some compound act as specific inhibitor of fungal cellular or metabolic process to inhibit the growth. Present researchers are focusing on identification of compounds that have specific and multiple inhibitors for fungal cellular process or pathogenicity related factors. Proteins that are responsible for the cellular process or pathogenicity of specific fungus would be the target for design of specific inhibitors that block the growth of the fungus. Like many other fungal pathogens *M. oryzae* infect host by elaborating a specialized infection cell called an appressorium. Melanin deposition in appresoria has been reported to contribute to rapture the host cell wall and establish host-pathogen interaction. Therefore, enzymes in the melanin biosynthetic pathway are valuable target for development of fungicides. Scytalone dehydratase, SDH1 (1STD), an enzyme involved in the melanin biosynthesis in may phytopathogenic fungi including *M. oryzae* [22]. SDH1 catalyzes the conversion of scytalone to 1, 3, 8-trihydroxynaphthalene, and vermelone to 1, 8-dihydroxynaphthalene. Whereas, trihydroxynaphthalene reductase, 3HNR (1YBV), an essential enzyme for the biosynthesis of fungal melanin, catalyzes the conversion of trihydroxynaphthalene to vermelone [23]. Subsequently, the 1, 8-dihydroxynaphthalene is polymerized into melanin. Moreover, during the morphogenesis of conidium to appresoriunm development, storage compounds like sugar and lipid present in the conidium are moved from conidium to appresorium as a source of energy required for generation of tugor pressure [24]. One such sugar, trehalose, is present in conidia of *M. oryzae* and is mobilized during appressorium formation. The biosynthesis of trehalose is partly regulated by trehalose-6-phosphate synthase, Tps1 (6JBI), and deletion of the *Tps1* gene in *M. oryzae* abolishes its ability to cause disease in rice [25–27]. Isocitrate lyase, ICL1 (5E9G), one of the principal enzymes of the glyoxylate cycle in the rice blast fungus *M. oryzae* helps cells to assimilate two-carbon compounds into the tricarboxylic acid cycle (TCA cycle) and channel these via gluconeogenesis to generate glucose. *Icl1* mutant cells impaired in germ tube emergence, appressorium development and cuticle penetration and were less virulent compared to wild type strain [28]. Recent study showed that bromophenols isolated from the red alga *Odonthalia corymbifera* exhibited potent ICL inhibitory activity and blocked appressoria formation by *M. grisea* as well as reduced disease severity was observed by the treatment of bromophenol in *M grisea* infected leaf [29].

Molecular docking and other computational study of inhibitors on their target enzymes/proteins of a pathogenic fungus can contribute a great help to estimate the potential of the inhibitors that could prevent the activity of an enzyme. *In silico* analyses of molecular docking and protein – ligand interaction of antifungal metabolites on target enzymes or proteins are also important for understanding the mechanism of antifungal action and their potential as a novel candidate fungicide against *M. oryzae*. In this study, we aimed to screen some recently reported inhibitory natural products against blast fungus *M. oryzae* for understanding their mechanisms of action and promise as candidate fungicides using *in silico* molecular docking studies on some enzymes involved in pre-infectional development of the blast fungus. The specific objectives of this study were

to (i) virtual screening and molecular docking simulation of 39 promising antifungal natural products on four enzymes viz. SDH1, 3HNR, TPS1 and ICL1 using PyRx 0.8, ii) assess fungicide-likeness, and iii) bioactivity of natural compounds using *in silico* analysis.

2. Results

2.1. Molecular docking simulations study

Molecular docking simulations were used to clarify the compounds' binding mode and obtain other information that could be utilized for further structural optimization [30,31]. Our selected compounds and two reference fungicide compounds were docked against the four different target enzymes Scytalone dehydratase or SDH1 (1STD), Trihydroxynaphthalene reductase (1YBV), trehalose-6-phosphate synthase 1 or Tps1 (6JBI) and isocitrate lyase enzyme or ICL1 (5E9G). The docked compounds were ranked based on the maximum occupancy of binding pocket with minimum free energy, the strength of hydrogen bonding, and other potential non-covalent interactions. Out of 39 docked molecules, top-ranking docking poses were selected. Protein-ligand binding affinity is essential for biological processes, as these physical and chemical interactions determine biological recognition at the molecular level. In this way, it is possible to look for a ligand capable of inhibiting or activating a specific target protein through its interaction. Therefore, it is crucial to find a ligand that binds to a target protein with high affinity [32]. The ranking criteria involved Lipinski's rule of five, the number of hydrogen bond interactions and binding with the selected protein targets involving the binding pocket residues.

Compounds were docked with two enzymes of the melanin pathway, Scytalone dehydratase (1STD) and Trihydroxynaphthalene reductase (1YBV), to inhibit the melanin pathway is responsible for appressorium formation (**Table S1**). Compound Cryptocin, HDFO, Tanzawaic-acid-L and Camptothecin showed strong binding affinity − 10.1 kcal/mol, -9.3 kcal/mol, -9.2 kcal/mol and − 9.1 kcal/mol respectively against Scytalone dehydratase (1STD) (Table 1A).

Cryptocin was bound with Scytalone dehydratase (1STD) and formed a hydrogen bond with side chain A:TYR50, whereas hydrophobic interactions with residues A:LEU76, A:PRO149, A:ILE151, A:VAL70, A:VAL75, A:LEU54, A:MET69, A:TYR50, A:PHE53, A:HIS85, A:PHE158, A:PHE169 (Table 1A **and** Fig. 1A). Rest of the compounds were interactions with amino acid residues A:SER129, A:TYR50, A:VAL75, A:PRO149, A:VAL70, A:LEU54, A:ARG166, A:TYR30, A:PHE53, A:PHE158, A:PHE162, A:PHE169, A:HIS85, A:VAL108, A:TRP26, A:HIS110 (Table 1A **and** Fig. 1B). Bond distance and type of interactions were shown in Table 2 **and Table S2**.

All these compounds showed strong binding with Scytalone dehydratase (1STD) active site residues followed by Tanzawaic-acid-L, Camptothecin, and HDFO, whose binding affinity was lower than Cryptocin. On the other hand, compounds Camptothecin, GKK1032A2, Alternariol-monomethyl-ether, Arohynapene-A, and Tricyclazole exhibit the highest binding affinity − 9.5 kcal/mol, -9.5 kcal/mol − 8.9 kcal/mol, -8.7 kcal/mol and − 8.3 kcal/mol, respectively with Trihydroxynaphthalene reductase (1YBV) amongst all compounds (Table 1B). Camptothecin showed hydrogen bond with residues B:GLY210, B:TYR223, B:MET215, B:THR213, and B:SER164 hydrophobic non bonded interactions are formed with B:GLY40, B:ILE41, B:MET215 and B:ARG39 and other bonds are B:MET215 and B:MET162 (Table 1B **and** Fig. 2B). Other compounds showed interaction

with B:TYR178, B:LYS182, B:THR213, A:ASN265, B:SER164, B:ILE41, B:ILE211, B:PRO208, B:MET162, A:ALA15, A:PRO17, A:LYS200, B:ARG248, B:LEU246, B:TYR223, B:CYS220, B:MET215, B:VAL219, B:ILE211, B:TYR216, B:TRP243, B:GLY209, B:GLY210, B:MET215 and B:MET283 as details shown in Table 1B and interaction of compound Alternariol-monomethyl-ether shown in Fig. 2A,B.

Bond distance and type of interactions were shown in Table 2 **and Table S2**. Camptothecin showed the highest binding affinity and more hydrogen bonds than other compounds, and all interactions are possessed in the active site residues of the protein. Likewise, in trehalose-6-phosphate synthase 1 or Tps1 (6JBI), the compound GKK1032A2, camptothecin, chaetoviridin-A and rocaglaol have been observed to bind through meaningful bonds having binding scores of -10.2 kcal/mol, -8.9 kcal/mol, -8.5 kcal/mol, and − 8 kcal/mol respectively (Table 1C). Hydrogen bonds favor the docking interactions of GKK1032A2 with A:MET390, A:HIS181, and A:LYS294, while non-bonded hydrophobic interactions are favored by A:LEU392, A:VAL393, and A:HIS181 (Table 1C **and** Fig. 3A). Other three compounds showed interactions with residues A:ASN21, A:ARG22, A:TYR99, A:HIS152, A:ARG327, B:LYS294, B:ASN391, B:VAL393, B:VAL287, A:THR46, A:HIS155, A:ASP153, A:TRP108, A:HIS112, A:HIS181, B:LEU371, B:LEU392, B:VAL324, A:HIS181, A:PRO24, A:LEU44, A:LEU48, as detailed in Table 1C and compound Camptothecin illustrated in Fig. 3B. Bond distance and type of interactions were shown in Table 2 **and Table S2**. GKK1032A2 showed strong binding with trehalose-6-phosphate synthase 1 or Tps1 (6JBI) active site residues and highest binding affinity compared to chaetoviridin-A, camptothecin and rocaglaol.

In case of the isocitrate lyase enzyme (5E9G), arohynapene-B and pannellin possess the highest binding affinity − 8.3 kcal/mol and − 8 kcal/mol, respectively amongst all the compounds (Table 1D). The binding conformations were analyzed, and we identified that arohynapene-B formed a hydrogen bond with A:ALA396, A:ALA399 and A:TYR38. In addition, several residues A:PRO397, A:PRO426, A:TYR38, A:TYR425 formed hydrophobic interactions (Table 1D **and** Fig. 4A). While pannellin formed hydrogen bond with A:LYS135, B:LYS135 and A:ASN134 and hydrophobic interactions with residues A:LYS135 and A:HIS138 whereas electrostatic interaction with A:ASP118 (Table 1D **and** Fig. 5B). Bond distance and type of interactions were shown in Table 2 **and Table S2.**

2.2. Fungicides likeness

Physicochemical properties of the potential compounds were analyzed to evaluate their fungicide-likeness nature. We analyzed the fungicide-likeness of the natural compounds under the well-established fundamental rule of drug-likeness i.e. Lipinski rule of 5. Natural compounds physicochemical properties include molecular weight, number of rotatable bonds, number of hydrogen bond acceptors, and number of hydrogen bond donors, topological polar surface area, Fraction Csp3, Molar refractivity, and Synthetic accessibility were analyzed. The predicted results were listed in Table 3. Interestingly all selected natural compounds bear the Molecular Weight range from 189.24 to 434.48 (< 500) except GKK1032A2 and pannellin. The milogP values of the potential compounds were found to be below 5 (0.89to 5.08) except compound GKK1032A2. According to Lipinski's rule, that most "drug-like" molecules have number of hydrogen bond acceptors ≤ 10, and number of hydrogen bond donors ≤ 5. Furthermore, the number of hydrogen bond donors was less than five, and the number of hydrogen bond acceptors was less than 10. Besides, TPSA of all potential compounds was observed in the range 46.53 to 112.91 Å².

2.3. Bioactivity score assessment of selected potential natural products

The bioactivity score of the selected compound was predicted through the Molinspiration server. In this prediction, biological activity measured by the bioactivity score for enzyme inhibitor was evaluated enzyme (Table 4), which are classified into three different ranges: molecule having bioactivity score greater than 0.00 is most likely to illustrate meaningful biological activity, while scores extending from − 0.50 to 0.00 are expected to be moderately active, and if the score is less than − 0.50, it is presumed to be inactive. The bioactivity scores for the G protein-coupled receptor ligand (GPCR) are most active for all the selected compounds except alternariol-monomethyl-ether and GKK1032A2 are moderately active, whereas tricyclazole is biologically inactive. Meanwhile, the ion channel modulators' scores for the tanzawaic-acid-L, arohynapene-B, HDFO, azoxystrobin, and strobilurin are biologically active, and all other compounds are moderately active except tricyclazole is biologically inactive.

The result of kinase inhibitors scores for the compound camptothecin and azoxystrobin have biological active score values, and other compounds are moderately active, whereas the compound GKK1032A2 and tricyclazole are inactive. Moreover, the nuclear receptor score values, all the compounds are biologically active, whereas tricyclazole is biologically inactive according to the classification ranges of Linn et al. [33]. Compounds alternariol-monomethyl-ether, tanzawaic-acid-L, arohynapene-A, camptothecin, pannellin, azoxystrobin, and strobilurin have moderately active score values; meanwhile, cryptocin, chaetoviridin-A, GKK1032A2, arohynapene-B, rocaglaol, and HDFO are biologically active, whereas compound Tricyclazole is inactive for Protease inhibitors. The structures of all compounds have score values for enzyme inhibitors greater than 0.00 considered biologically active. Meanwhile, the compound pannellin has moderately active score values, whereas the compound tricyclazole has inactive score values.

3. Discussion

Blast caused by *M. oryzae* is a destructive disease of cereal crops that causes enormous economic losses by reducing the grain yield [18]. Although the chemical fungicides provide a marginal protection against blast disease but increasing risk of health hazard and pathogen resistant is a matter of concern. Hence there is still a need to discover some alternative natural fungicides against *M. oryzae* infection that can be more effective as they will be environmentally suitable with less toxicity. To find out potential fungicides against *M. oryzae*, we performed a literature-based survey and identified 12 compounds that differently inhibit the growth of *M. oryzae* fungus. Molecular docking study revealed that most of these compounds bind either 1STD or 1YBV or 6JBI and/or 5E9G enzymes responsible for either melanin biosynthesis or appresoria formation enzymes of *M. oryzae*. Scytalone dehydratase, SDH1 (1STD) and Trihydroxy naphthalene reductase, 3HNR (1YBV), two key enzymes of melanin biosynthesis pathway and found to be essential for virulence in plant pathogenic fungi [22,34]. Various studies have reported that the SDH1 and 3HNR enzymes are promising molecular target for the identification of potential inhibitors [35,36]. Up to date several synthetic fungicides namely, carpropamid, tricyclazole, pyroquilon and phthalide have been discovered that inhibit these two enzymes of melanin biosynthesis pathway. Although these compounds were effective against *M. oryzae* but extensive uses of these fungicides lead to development of resistance. For instance, carpropamid, ((1RS,3SR)-2,2-dichloro-N-

[(R)-1- (4-chlorophenyl)ethyl]-1-ethyl-3-methylcyclopropanecarboxamide), a commercial fungicide, that targets the scytalone dehydratase enzyme and it has been widely used in Japan as the chemical agent for nursery-box treatment against leaf blast of rice [16]. However, a single-point mutation in *Sdh1* in *M oryzae* isolates causing substitution of one amino acid in the scytalone dehydratase gene showing decreased sensitivity to carpropamid [37].

Two other enzymes namely trehalose-6-phosphate synthase, TPS1 (6JBI), Isocitrate lyase, ICL1 (5E9G), have also been shown are good targets to design fungicides. TPS1 is the key enzyme in trehalose biosynthetic pathways that catalyzes the transfer of glucose from uridinediphospho (UDP)-glucose to glucose 6-phosphate to generate trehalose 6-phosphate (T6P). TPS1 appeared to be dispensable for development and virulence *M. oryzae*, *Fusarium verticillioides*, *Puccinia striiformis* f. sp. *tritici* and *Fusarium graminearum* and *Tps1* mutants showed reduced pathogenicity [38,39]. Since fungal TPS1 shares minimal similarity to plant homologs therefore, inhibition of TPS1 may serve as a promising target for the development of new strategies to control fungal diseases [40]. As for example, Validamycin A, a competitive inhibitor of Tps1 and have been used as potential fungicide [41]. Isocitrate lyase (ICL), a key enzyme in carbon metabolism and is essential for the pathogenesis for both human and plant fungal pathogens [42]. It has been shown that *icl*1 gene of *Leptosphaeria maculans* involved in successful host colonization of *Brassica napus*, whereas an *M. grisea Icl*1 regulates virulence-associated functions such as germ tube emergence, appressorium development, and cuticle penetration. Δ*icl* mutants exhibits less virulent than wild type and impaired virulence-associated function [43]. Several natural compounds have been identified as inhibitor of *Icl*1. Halisulfate 1, a sesterterpene sulfate, isolated from tropical sponge *Hippospongia* spp., reduces both appresorium formation and infection of rice plants by the fungus *M. grisea* by potentially binding with *Icl*1 [43]. Bromophenols, another natural compound isolated from the red alga *Odonthalia corymbifera* exhibited potent ICL inhibitory activity and blocked appresoria formation of *M. grisea* in a concentration-dependent manner [29]. Joshi et al. [44] used ICL as a molecular target to discover new antifungal compounds against *F. graminarearum* using molecular dynamic study. Four natural compounds namely, Melianoninol, Nimbinene, Vilasinin, and Fraxinellone from *Melia azedarach* identified as potent inhibitor of *ICL*1. Molecular dynamics simulation demonstrated that these four phytochemicals displayed considerable significant structural and pharmacological properties and could be probable antifungal drug candidates against *F. graminarearum*. Therefore, molecular docking and simulations studies could be utilized to predict the efficiency of binding of the ligand with biomolecules [45,46].

In this study, a total of 39 compounds were subjected to molecular docking study and 12 of them showed good binding affinity with the aforementioned four enzymes of *M. oryzae*. Among the 12 compounds, four compounds viz. cryptocin, tanzawaic-acid-L, camptothecin, and HDFO strongly bind with 1STD whereas five natural compounds namely, alternariol-monomethyl-ether, GKK1032A2, arohynapene-A, camptothecin, and tricyclazole strongly bind with trihydroxy naphthalene reductase (1YBV). Chaetoviridin-A, GKK1032A2, camptothecin, and rocaglaol showed strong binding affinity for 6JBI whereas, only two compounds viz. arohynapene-B and pannellin were bind with 5E9G with less energy requirement. Then, we have subjected the all the compound for analyzing fungicide-likeness by the Lipinski's rule of 5. According to Lipinski's rule of 5, a compound would be an active fungicide if it satisfies all the properties of pharmacological and biological activity. Molecular weight of a chemical is an important criterion to determine its fungicides activity. The molecules that have low molecular weight (≤500) are readily transported, diffused and absorbed by the cell

membrane in comparison to large molecules [47]. Molecular weight of the selected compounds was found more or less than 500 g/mol (189.24 g/mol to 506.5 g/mol). In addition, the positive Log*P* values indicate easier passage of compounds through bio-membranes and the acceptable limit is ≤5 [48,49]. Moreover, the lipophilic compounds easily permeable trough cell membrane by passive diffusion and bind with biomolecules to inhibit the vital metabolic enzymes in to the cell. Therefore, the membrane permeability depends on the lipophilic nature of a compound. The calculated log P value of natural compounds was ranging from 0.89 to 5.08 which is ideal for crossing the cell membrane. Recently, Steinberg et al. [50] reported that C_{18}-SMe_2^+, a mono-alkyl lipophilic cations (MALCs) having Log*P* value 2.26 easily diffuse through plasma membrane. Although molecular weight and logP value of some compounds were exceed the expected limit mentioned in Lipinski's rule 5 but it would be worth mentioning that this slight increase in molecular weight and milogP value will not have a significant impact on compound transportation and diffusion. It has been shown that the molecular mass of several FDA-approved drugs was more significant than 500 g/mol [51]. Furthermore, the number of hydrogen bond donors was less than five, and the number of hydrogen bond acceptors was less than 10 [52]. Besides, TPSA of all potential compounds was observed in the range 46.53 to 112.91 Å² which is also between the acceptable ranges (Lipinski 2004). In case of bioactivity score, all the compound poses a score value of −0.50 to 0.00 which indicate the compounds are biologically active except tricyclazole.

Among the compounds, camptothecin, a very well-known alkaloid isolated from plant origin showed strong binding affinity with 1STD, 1YBV and 6JBI. As evident in several reports camptothecin treatment inhibits the growth of *M. oryzae*, *Rhizoctonia solani*, *Alternaria alternata*, *Colletotrichum gloeosporioides*, *Fusarium oxysporum*, *Botrytis cinerea*, *Sphaerotheca fuliginea* and *Pseudoperonospora cubensis* [1,53]. Among the reported fungi, camptothecin was found to be most effective against *M. oryzae*, at a concentration 1.53 µg/mL (EC50 value) whereas, it was effective against mycelial growth of *A. alternate* and *F. oxysporum* with EC50 value 250 µg/ mL and for *C. gloeosporioides*, it was 500µg/mL. The molecular simulation result showed that CPT could binds to the interface of DNA-topoisomerase I complex of *M. oryzae* and affecting the translation and carbohydrate metabolism/energy metabolism leading to cell death [53]. Four other natural compounds namely, GKK1032A2 tanzawaic-acid-L, arohynapene-A and arohynapene-B were identified from fungus *Penicillium* sp. showed conidial germination inhibition in *M. oryzae* [54]. While the compound GKK1032A2 was effective at a concentration 3 µg/mL, the rest of the compounds were effective at 25–50 µg/mL. However, GKK1032A2 has been found to be ineffective against other phytopathogenic fungi including *F. graminearum*, *B. cinerea* and *P. infestans* but the antifungal activity of tanzawaic-acid-L arohynapene-A and arohynapene-B on other phytopathogenic fungus have not been tested yet. Interesting, HDFO, (3aS,4aR,8aS,9aR)-3a-hydroxy-8a-methyl-3,5-dimethylenedecahydronaphto [2,3-b]furan-2(3H)-one, a newly identified compound from *Biscogniauxia* sp. O821 completely inhibited condial germination of *M oryzae* at a concentration of less than 5 ppm whereas blast lesion formation was significantly reduced in the presence of 5 and 10 ppm HDFO. In addition, this compound had antifungal activity against *A. alternata*, *Cochliobolus miyabeanus*, *Colletotrichum orbiculare*, *Corynespora cassiicola*, *Fusarium oxysporum* f.sp. *conglutinans* and *Fusarium oxysporum* f.sp. *spinaciae* at > 50 ppm [55]. Like as HDFO, cryptocin also inhibit the growth of a wide range of fungi including *M. oryzae* with Minimum Inhibitory Concentration (MIC) value less than 1.0 µg/mL [20]. Engelmeier et al. [56] reported rocaglaol and pannellin inhibit germ tube formation at 1.6 and 3 µg/mL respectively. Therefore, all the 12

compounds could be used as lead compound or biofungicide for the inhibition of aforementioned enzymes in *M. oryzae*.

Although there are a number of fungicides are available for the control of many diseases, the blast disease caused by the different pathotypes of *M. oryzae* remain to be managed effectively. Recent studies suggest that most of the important plant pathogenic fungi acquired resistance against chemical fungicides [57,58]. Currently used fungicides generally target a single enzyme which can be overcome by single point mutation [17,37]. For instance, extensive use of strobilurin (QoI) fungicides in Brazil has led to a widespread distribution of cyt b mutations conferring resistance in strains isolated from wheat and other grasses [17]. Therefore, an alternative approach such as multi-site mode of action fungicides are needed to be discovered for the management of devastative blast disease. It is hypothesized that fungicides with multi-site mode of action would not be easily overcome by the emergence of resistance [58]. In the current study we identified three natural products viz. camptothecin, GKK1032A2 and arohynapene-A have multiple enzymes target for inhibition of blast fungus. Therefore, these compounds merit further study in vivo evaluation for considering them as potential fungicides or lead compound to control blast disease.

4. Conclusions

The control of blast diseases in major cereal crops viz. rice, wheat, maize etc. using natural compounds is an advanced and risk-free method for disease management in agriculture. The results of present study clearly revealed that the camptothecin, GKK1032A2 and arohynapene-A could act as potential lead compounds for the development of effective fungicides against the most notorious blast fungus. All these compounds showed greatest binding affinity more than one target proteins along with a good number of H-bond and bioactivity score compared to the currently available fungicide for blast disease management. These compounds hold ideal logP values and low molecular weights. Therefore, these compounds could cross the cell membranes and are able to inhibit the target enzymes in *M. oryzae* that involved in pathogenesis related factors in blast fungus. Our results convincingly suggest that at least three antifungal natural compounds viz. camptothecin, GKK1032A2 and arohynapene-A target multiple enzymes involved in melanin biosynthesis and appressoria formation in the blast fungus *M. oryzae*. Both these processes are essential for successful infection of host plants by the *M. oryzae*. Further in vivo molecular and field study are required for confirming the findings of this *in silico* study before recommending camptothecin, GKK1032A2 and arohynapene-A as fungicides or lead compounds against *M. oryzae*.

5. Materials And Methods

5.1. Protein preparation

The crystal structure of *Magnaporthe oryzae* Scytalone dehydratase (PDB ID: 1STD at 2.90 Å resolution), Trihydroxynaphthalene reductase (PDB ID: 1YBV at 2.80 Å resolution), trehalose-6-phosphate synthase 1 (Tps1) (PDB ID: 6JBI at 2.50 Å resolution) and Isocitrate lyase (PDB ID: 5E9G at 2.10 Å resolution), was retrieved from Research Collaboratory for Structural Bioinformatics (RCSB) Protein Data Bank (PDB) [59] and considered as a template for all molecular docking simulation. **For protein preparation, we used Discovery Studio 2019 molecular visualization software 4.5 [60] and PyMOL 2.3.3 software [61]. First, the proteins were**

uploaded to the software and found unnecessary objects such as default given ligands, ions, and water molecules were removed from the PDB file. Finally, the files were saved in PDB file format for further analysis. List of the enzymes/proteins and their biological functions are given in spplementary Table 1.

5.2. Ligand dataset preparation

The canonical smiles of 39 compounds were retrieved from the PubChem database [62], and their 3D structures were generated using Online SMILES Translator and Structure File Generator [63]. Afterward, each of the compounds was ready as ligands for molecular docking study with the target proteins. The 2D chemical structure of best-docked compounds is illustrated in **Fig. 5.**

5.3. Molecular docking simulation

In structural biology, molecular docking is a well-known and reliable technique, especially in computer-aided drug design (CADD) processes [64]. The technique ensures the best prediction of binding mode between a small molecule and a specific macromolecule [65]. The active site of the proteins was identified before going to the molecular docking simulation study through metaPocket (https://projects.biotec.tu-dresden.de/metapocket/) and cross-checked by another server named CASTp (http://sts.bioe.uic.edu/castp/index.html?2r7g). Molecular docking simulation was carried out using PyRx 0.8 virtual screening software [66]. For simulating the best interaction, the docking was performed setting the center in axis x- 32.0745, axis y- 36.2698 and axis z- 17.8046 with the dimension was in axis x- 38.0525 Å, axis y- 33.7716 Å and axis z- 51.7508 Å for Scytalone dehydratase (PDB ID: 1STD); center in axis x- 71.3457, axis y- 13.7945 and axis z- 31.7174 with the dimension was in axis x- 70.3723 Å, axis y- 60.4891 Å and axis z- 66.3320 Å for Trihydroxynaphthalene reductase (PDB ID: 1YBV); center in axis x- 23.3577, axis y- (-0.9662) and axis z- 25.0398 with the dimension was in axis x- 61.2168 Å, axis y- 98.7383 Å and axis z- 95.6880 Å for Tps1 (PDB ID: 6JBI); center in axis x- (-21.315), axis y- 34.7671 and axis z- 30.1677 with the dimension was in axis x- 147.9292 Å, axis y- 83.7344 Å and axis z- 82.9492 Å for Isocitrate lyase enzyme (PDB ID: 5E9G).. After docking simulation, the protein data bank partial charge & atom type (pdbqt) file format, given by PyRx as output, was saved for further protein-ligand interaction analysis.

5.4. Protein-ligand interaction analysis

For a clear view of protein-ligand interaction of the best-docked complexes, 2D plots of protein-ligand interactions were analyzed through Discovery Studio 4.5. It generates a 2D graph of hydrogen bonds, electrostatic interactions, and hydrophobic interactions, contributing to the affinity of the drug-like molecules within the active site of ***M. oryzae*** proteins.

5.5. Fungicides likeness

The physicochemical parameters of the most promising compounds were predicted using the web tool SwissADME (http://www.swissadme.ch/index.php). The predicted parameters included the number of rotatable bonds, number of hydrogen bond acceptors, number of hydrogen bond donors, partition coefficient log p (miLog P), molecular weight, synthetic accessibility, and topological polar surface area (TPSA).

5.6. Bioactivity score prediction

The online Molinspiration Cheminformatics server (http://www.molinspiration.com) was utilized to evaluate the biological activity of selected compounds. The prediction was based on the enzyme inhibition score such as G-protein-coupled receptor (GPCR), Ion channel modulator, Kinase inhibitor, Nuclear receptor ligand, Protease inhibitor, and Enzyme inhibitor. The results are calculated according to previously published recommendations [33]. Therefore, it is recommended that if the value is equal to or greater than 0.00, the more active it will be, while if the values are between -0.50 and 0.00, it is moderately active, and, if the score is less than -0.50, it will be considered inactive [67,68].

Tables

e 1: Summary of top-ranked compounds screened against Scytalone dehydratase (1S ydroxynaphthalene reductase (1YBV), trehalose-6-phosphate synthase 1 or Tps1 (6JBI) and isoci e enzyme (5E9G) with their respective binding energy and interacting amino acid residues.

ounds	Binding Energy (kcal/mol)	Residues involved in Hydrogen bond Interaction	Residues involved in Hydrophobic interaction	Electrostatic interaction	Other
STD					
ocin	-10.1	A:TYR50	A:LEU76, A:PRO149, A:ILE151, A:VAL70, A:VAL75, A:LEU54, A:MET69, A:TYR50, A:PHE53, A:HIS85, A:PHE158, A:PHE169		
waic-	-9.2	A:SER129	A:VAL75, A:PRO149, A:VAL70, A:LEU54, A:ARG166, A:TYR30, A:TYR50, A:PHE53, A:PHE158, A:PHE162, A:PHE169		
tothecin	-9.1	A:TYR50	A:HIS85, A:PRO149, A:LEU54, A:TYR50, A:PHE53		
	-9.3	A:TYR50	A:PRO149, A:VAL108, A:TRP26, A:TYR30, A:HIS85, A:HIS110, A:PHE158		
ence ystrobin)	-7	A:GLN84	A:TYR24, A:MET20, A:TYR16, A:TRP92, A:ALA27, A:ILE87, A:VAL23		A:MET20
ence ilurin)	-6.9	A:LYS148	A:LEU132, A:ALA130, A:ILE101, A:TYR103, A:TRP134	A:ASP150	
ZBV					
ariol- methyl-	-8.9	B:TYR178, B:LYS182, B:GLY210, B:THR213, B:PRO208,	B:MET215, B:ILE41, B:ILE211, B:PRO208, B:MET162		B:MET215
032A2	-9.5	A:ASN265	A:ALA15, A:PRO17, A:LYS200, B:ARG248, B:LEU246		
napene-	-8.7	B:THR213, B:TYR223	B:TYR223, B:CYS220, B:MET215, B:VAL219, B:ILE211, B:TYR216, B:TRP243		B:MET283
tothecin	-9.5	B:GLY210, B:TYR223, B:MET215, B:THR213, B:SER164	B:GLY40, B:ILE41, B:MET215, B:ARG39		B:MET21, B:MET162
lazole	-8.3	B:SER164, B:TYR178, B:TYR223	B:TYR223, B:GLY209, B:GLY210, B:MET215, B:VAL219		B:CYS220, B:MET283
ence	-8.9	B:ARG39,	B:ILE41, B:MET215,		

ystrobin)		B:ALA61, B:ASN62, B:SER63, B:MET215, B:GLY36, B:ILE41	B:ALA61		
ence ilurin)	-7.4	B:VAL274	B:ARG190, B:ALA207, B:LYS273, B:ILE165, B:VAL274		
BI					
oviridin-	-8.5	A:ASN21, A:ARG22, A:TYR99, A:HIS152, A:ARG327	A:TRP108, A:HIS112, A:HIS152, A:HIS181	A:ASP153	
032A2	-10.2	A:MET390, A:HIS181, A:LYS294	A:LEU392, A:VAL393, A:HIS181		
tothecin	-8.9	B:LYS294, B:ASN391, B:LEU392, B:VAL393, B:VAL287	B:LEU371, B:LEU392, B:VAL324		
laol	-8	A:THR46, A:HIS155, A:ASP153, A:TYR99	A:HIS152, A:HIS155, A:HIS181, A:PRO24, A:LEU44, A:LEU48, A:ARG22, A:TYR99, A:TRP108	A:ASP153	
ence ystrobin)	-7.8	A:ARG289, A:LYS294, A:ASP288, A:ASP153	A:HIS181, A:TRP108, A:TYR154, A:HIS155, A:VAL393		
ence bilurin)	-7.4	B:ASN100, B:TYR154, B:ARG327, B:ARG22, B:TYR99	B:TYR99, B:ALA95, B:ARG327, B:TRP62		
E9G					
napene-	-8.3	A:ALA396, A:ALA399, A:TYR38	A:PRO397, A:PRO426, A:TYR38, A:TYR425		
llin	-8	A:LYS135, B:LYS135, A:ASN134	A:LYS135, A:HIS138,	A:ASP118	
ence ystrobin)	-7	A:LYS214	A:LEU124, B:ALA517, B:VAL520, B:LYS525		B:ASP521
ence ilurin)	-6.7	A:LYS214, A:ARG380, B:ASP521	A:LEU260, A:LEU124, A:LYS214, A:MET218		

*Active site amino acids are bolded

Table 2: Type of interactions, interacting residues and bond distance of Scytalone dehydratase (1STD), Trihydroxynaphthalene reductase (1YBV), trehalose-6-phosphate synthase 1 or Tps1 (6JBI) and isocitrate lyase enzyme (5E9G) with their best binding energy compound.

Compounds	Interacting amino acid residues	Bond distance (Å)	Interaction category	Type of Interaction
1YBV vs. Camptothecin	B:ARG39	5.35551	Hy Bond	Pi-Alkyl
	B:GLY40	3.84091	Hy Bond	Pi-Sigma
	B:ILE41	3.34078	Hy Bond	Pi-Sigma
	B:MET162	5.34854	Other	Pi-Sulfur
	B:SER164	3.32811	H Bond	Carbon H Bond
	B:GLY210	3.07126	H Bond	Conventional H Bond
	B:THR213	2.77025	H Bond	Conventional H Bond
	B:MET215	2.23423	H Bond	Conventional H Bond
	B:MET215	5.16755	Hy Bond	Alkyl
	B:MET215	3.14003	Other	Sulfur-X
	B:TYR223	3.14331	H Bond	Conventional H Bond
1STD vs. Cryptocin	A:TYR50	2.95919	H Bond	Conventional H Bond
	A:TYR50	5.36041	Hy Bond	Pi-Alkyl
	A:PHE53	4.93096	Hy Bond	Pi-Alkyl
	A:LEU54	4.45416	Hy Bond	Alkyl
	A:VAL70	4.64779	Hy Bond	Alkyl
	A:VAL75	4.05694	Hy Bond	Alkyl
	A:LEU76	5.39137	Hy Bond	Alkyl
	A:MET69	4.3566	Hy Bond	Alkyl
	A:HIS85	4.83013	Hy Bond	Pi-Alkyl
	A:PRO149	4.08713	Hy Bond	Alkyl
	A:ILE151	4.81867	Hy Bond	Alkyl
	A:PHE158	4.80565	Hy Bond	Pi-Alkyl
	A:PHE169	4.43414	Hy Bond	Pi-Alkyl
5E9G vs. Arohynapene-B	A:TYR38	3.35874	H Bond	Carbon H Bond
	A:TYR38	5.23978	Hy Bond	Pi-Alkyl
	A:ALA396	2.1551	H Bond	Conventional H Bond
	A:PRO397	4.70296	Hy Bond	Alkyl
	A:ALA399	2.88171	H Bond	Conventional H Bond
	A:TYR425	5.1667	Hy Bond	Pi-Alkyl
	A:PRO426	4.49266	Hy Bond	Alkyl
6JBI vs. GKK1032A2	A:HIS181	1.9225	H Bond	Conventional HBond
	A:HIS181	4.23591	Hy Bond	Pi-Alkyl
	A:LYS294	3.41725	H Bond	Pi-Cation
	A:MET390	2.66371	H Bond	Conventional H Bond
	A:LEU392	4.53888	Hy Bond	Alkyl
	A:VAL393	5.01831	Hy Bond	Alkyl

H= Hydrogen, Hy= Hydrophobic

Table 3: Physicochemical properties of selected potential compound and reference fungicide compound.

Compound	MW (g/mol)	RB	HBA	HBD	miLogP	Lipinski	TPSA (Å)	Synthetic accessibility
Alternariol-monomethyl-ether	272.25	1	5	2	2.74	Yes	79.9	2.83
Cryptocin	361.48	3	4	1	0.89	Yes	74.68	4.76
Chaetoviridin-A	432.89	6	6	1	3.22	Yes	89.9	5.68
GKK1032A2	503.67	1	2	4	5.08	Yes	75.63	7.28
Tanzawaic-acid-L	288.38	3	3	2	3.19	Yes	57.53	5.16
Arohynapene-A	286.37	3	3	2	3.12	Yes	57.53	4.12
Arohynapene-B	286.37	4	3	2	3	Yes	57.53	4.01
Camptothecin	348.35	1	5	1	2.03	Yes	81.2	3.84
Rocaglaol	434.48	5	6	2	4.48	Yes	77.38	4.85
Pannellin	506.5	6	9	2	4.28	Yes	112.91	5.35
Tricyclazole	189.24	0	2	0	2.4	Yes	58.43	2.44
HDFO	248.32	0	3	1	1.51	Yes	46.53	4.02
Azoxystrobin	403.39	8	8	0	3.38	Yes	103.56	3.42
Strobilurin	442.5	6	7	1	4.92	Yes	83.45	5.6

MW- Molecular weight, RB- Rotatable Bond, HBA- Hydrogen bond acceptor, HBD- Hydrogen bond donor, TPSA- Topological surface area.

Table 4: Prediction of bioactivity of the selected compounds and reference fungicide compounds.

Compounds	GPCR ligand	Ion channel modulator	Kinase inhibitor	Nuclear receptor ligand	Protease inhibitor	Enzyme inhibitor
Alternariol-monomethyl-ether	-0.41	-0.44	-0.25	0.23	-0.48	0.03
Cryptocin	0.08	-0.25	-0.48	0.2	0.24	0.18
Chaetoviridin-A	0	-0.35	-0.44	0.09	0.02	0.28
GKK1032A2	-0.16	-0.17	-0.76	0.13	0.07	0.05
Tanzawaic-acid-L	0.17	0.03	-0.47	0.61	-0.11	0.41
Arohynapene-A	0.36	-0.01	-0.17	0.41	-0.05	0.29
Arohynapene-B	0.29	0.12	-0.22	0.3	0.08	0.35
Camptothecin	0.46	-0.15	0.27	0.07	-0.1	1.11
Rocaglaol	0.18	-0.01	-0.1	0.4	0.01	0.1
Pannellin	0.08	-0.15	-0.29	0.35	-0.04	-0.01
Tricyclazole	-1.23	-0.74	-0.73	-2.08	-1.89	-0.63
HDFO	0.14	0.13	-0.25	0.87	0.03	0.69
Azoxystrobin	0.25	0.03	0.09	0.25	-0.12	0.19
Strobilurin	0.27	0	-0.17	0.51	-0.03	0.17

Supplementary Tables

Table S1: Type of interactions, interacting residues and bond distance of Scytalone dehydratase (1STD), Trihydroxynaphthalene reductase (1YBV), trehalose-6-phosphate synthase one or Tps1 (6JBI), isocitrate lyase enzyme (5E9G), with the selected fungicide compound.

Compounds	Interacting amino acid residues	Bond distance (Å)	Interaction category	Type of Interaction
1STD vs. Azoxystrobin	A:TYR16	5.1848	Hy Bond	Pi-Alkyl
	A:MET20	4.64773	Hy Bond	Alkyl
	A:MET20	5.62552	Other	Pi-Sulfur
	A:VAL23	5.4992	Hy Bond	Pi-Alkyl
	A:TYR24	4.70402	Hy Bond	Pi-Pi Stacked
	A:ALA27	4.6699	Hy Bond	Pi-Alkyl
	A:GLN84	3.23819	H Bond	Conventional H Bond
	A:ILE87	5.4548	Hy Bond	Pi-Alkyl
	A:TRP92	4.92997	Hy Bond	Pi-Alkyl
1STD vs. Strobilurin	A:ILE101	5.27854	Hy Bond	Alkyl
	A:TYR103	4.86174	Hy Bond	Pi-Alkyl
	A:ALA130	3.67326	Hy Bond	Alkyl
	A:LEU132	3.84036	Hy Bond	Pi-Sigma
	A:TRP134	4.93422	Hy Bond	Pi-Alkyl
	A:LYS148	2.80766	H Bond	Conventional H Bond
	A:ASP150	4.91626	Other	Pi-Anion
1YBV vs. Azoxystrobin	B:GLY36	2.69794	H Bond	Conventional H Bond
	B:ARG39	3.00579	H Bond	Conventional H Bond
	B:ILE41	4.12944	H Bond	Pi-Donor H Bond
	B:ILE41	4.66549	Hy Bond	Pi-Alkyl
	B:ALA61	3.12197	H Bond	Conventional H Bond
	B:ALA61	4.71583	Hy Bond	Pi-Alkyl
	B:ASN62	3.15534	H Bond	Conventional H Bond
	B:SER63	2.99912	H Bond	Conventional H Bond
	B:MET215	3.01993	H Bond	Conventional H Bond
	B:MET215	5.04026	Hy Bond	Pi-Alkyl
1YBV vs. Strobilurin	B:VAL274	4.10961	H Bond	Pi-Donor H Bond
	B:ARG190	5.32698	Hy Bond	Alkyl
	B:ALA207	3.68404	Hy Bond	Alkyl
	B:LYS273	4.84762	Hy Bond	Alkyl
	B:ILE165	4.87589	Hy Bond	Alkyl
	B:VAL274	4.85917	Hy Bond	Pi-Alkyl
6JBI vs. Azoxystrobin	A:TRP108	4.70808	Hy Bond	Pi-Pi T-shaped
	A:ASP153	3.54525	H Bond	Carbon H Bond
	A:TYR154	5.12316	Hy Bond	Pi-Alkyl
	A:HIS155	4.74001	Hy Bond	Pi-Alkyl
	A:HIS181	3.94673	Hy Bond	Pi-Sigma
	A:ASP288	3.10102	H Bond	Carbon H Bond
	A:ARG289	3.13091	H Bond	Conventional H Bond
	A:LYS294	2.97898	H Bond	Conventional H Bond
	A:VAL393	4.64628	Hy Bond	Pi-Alkyl
6JBI vs.	B:ARG22	4.17472	H Bond	Pi-Donor H Bond

Strobilurin	B:TRP62	4.86579	Hy Bond	Pi-Alkyl
	B:ALA95	4.10978	Hy Bond	Alkyl
	B:TYR99	3.94277	H Bond	Pi-Donor H Bond
	B:TYR99	5.74107	Hy Bond	Pi-Pi T-shaped
	B:ASN100	2.90799	H Bond	Conventional H Bond
	B:TYR154	2.89275	H Bond	Conventional H Bond
	B:ARG327	3.02748	H Bond	Conventional H Bond
	B:ARG327	4.56151	Hy Bond	Alkyl
5E9G vs. Azoxystrobin	A:LEU124	3.54711	Hy Bond	Pi-Sigma
	A:LYS214	3.1052	H Bond	Conventional H Bond
	B:ALA517	5.12416	Hy Bond	Pi-Alkyl
	B:VAL520	5.25347	Hy Bond	Pi-Alkyl
	B:ASP521	3.50407	Other	Pi-Anion
	B:LYS525	5.29024	Hy Bond	Pi-Alkyl
5E9G vs. Strobilurin	A:LEU124	4.76458	Hy Bond	Alkyl
	A:LYS214	3.19943	H Bond	Conventional H Bond
	A:LYS214	4.45867	Hy Bond	Alkyl
	A:MET218	4.54471	Hy Bond	Alkyl
	A:LEU260	4.93381	Hy Bond	Alkyl
	A:ARG380	3.49642	H Bond	Carbon H Bond
	B:ASP521	3.61028	H Bond	Carbon H Bond

H= Hydrogen, Hy= Hydrophobic

Table S2: Type of interactions, interacting residues and bond distance of Scytalone dehydratase (1STD), Trihydroxynaphthalene reductase (1YBV), trehalose-6-phosphate synthase 1 or Tps1 (6JBI), isocitrate lyase enzyme (5E9G), with the other selected compounds.

Compounds	Interacting amino acid residues	Bond distance (Å)	Interaction category	Type of Interaction
1STD vs. Tanzawaic-acid-L	A:TYR30	4.57912	Hy Bond	Pi-Alkyl
	A:TYR50	4.74722	Hy Bond	Pi-Alkyl
	A:PHE53	5.39016	Hy Bond	Pi-Alkyl
	A:LEU54	4.22005	Hy Bond	Alkyl
	A:VAL70	4.86485	Hy Bond	Alkyl
	A:VAL75	4.66304	Hy Bond	Alkyl
	A:SER129	2.46023	H Bond	Conventional H Bond
	A:PRO149	5.47299	Hy Bond	Alkyl
	A:PHE158	4.66232	Hy Bond	Pi-Alkyl
	A:PHE162	3.49342	Hy Bond	Pi-Alkyl
	A:ARG166	4.51563	Hy Bond	Alkyl
	A:PHE169	4.9856	Hy Bond	Pi-Alkyl
1STD vs. Camptothecin	A:TYR50	3.63955	H Bond	Pi-Donor H Bond
	A:TYR50	4.99408	Hy Bond	Pi-Alkyl
	A:PHE53	4.0495	Hy Bond	Pi-Alkyl
	A:LEU54	4.17104	Hy Bond	Alkyl
	A:HIS85	5.86733	Hy Bond	Pi-Pi T-shaped
	A:PRO149	4.97318	Hy Bond	Alkyl
1STD vs. HDFO	A:TRP26	5.07574	Hy Bond	Pi-Alkyl
	A:TYR30	5.18325	Hy Bond	Pi-Alkyl
	A:TYR50	2.91435	H Bond	Conventional H Bond
	A:HIS85	4.85989	Hy Bond	Pi-Alkyl
	A:VAL108	4.00524	Hy Bond	Alkyl
	A:HIS110	4.39831	Hy Bond	Pi-Alkyl
	A:PRO149	4.84767	Hy Bond	Alkyl
	A:PHE158	5.31703	Hy Bond	Pi-Alkyl
1YBV vs. Alternariol-monomethyl-ether	B:ILE41	4.74505	Hy Bond	Alkyl
	B:MET162	5.26285	Hy Bond	Pi-Alkyl
	B:TYR178	3.16042	H Bond	Conventional H Bond
	B:LYS182	3.13789	H Bond	Conventional H Bond
	B:PRO208	2.24883	H Bond	Conventional H Bond
	B:PRO208	4.76055	Hy Bond	Pi-Alkyl
	B:GLY210	3.32215	H Bond	Conventional H Bond
	B:ILE211	3.9343	Hy Bond	Alkyl
	B:THR213	2.95007	H Bond	Conventional H Bond
	B:MET215	3.68835	Hy Bond	Pi-Sigma
	B:MET215	4.10695	Other	Pi-Sulfur
1YBV vs. GKK1032A2	A:ALA15	5.06932	Hy Bond	Alkyl
	A:PRO17	5.2637	Hy Bond	Alkyl
	A:LYS200	5.3372	Hy Bond	Alkyl
	B:LEU246	4.53376	Hy Bond	Alkyl
	B:ARG248	3.92783	Hy Bond	Alkyl
	A:ASN265	2.36537	H Bond	Conventional H Bond

1YBV vs. Arohynapene-A	B:ILE211	5.15363	Hy Bond	Alkyl
	B:THR213	2.7626	H Bond	Conventional H Bond
	B:MET215	4.21542	Hy Bond	Alkyl
	B:TYR216	4.45903	Hy Bond	Pi-Alkyl
	B:VAL219	5.34854	Hy Bond	Alkyl
	B:CYS220	5.09712	Hy Bond	Alkyl
	B:TYR223	4.00308	H Bond	Pi-Donor H Bond
	B:TYR223	3.32618	Hy Bond	Pi-Sigma
	B:TRP243	4.58665	Hy Bond	Pi-Alkyl
	B:MET283	5.79345	Other	Pi-Sulfur
1YBV vs. Tricyclazole	B:SER164	1.80365	H Bond	Conventional H Bond
	B:TYR178	2.11557	H Bond	Conventional H Bond
	B:GLY209	4.39859	Hy Bond	Amide-Pi Stacked
	B:GLY210	4.39859	Hy Bond	Amide-Pi Stacked
	B:MET215	4.18564	Hy Bond	Alkyl
	B:VAL219	5.30239	Hy Bond	Alkyl
	B:CYS220	4.89439	Other	Pi-Sulfur
	B:TYR223	3.57611	H Bond	Pi-Donor H Bond
	B:TYR223	4.03173	Hy Bond	Pi-Pi Stacked
	B:MET283	5.37817	Other	Pi-Sulfur
6JBI vs. Chaetoviridin-A	A:ASN21	2.97488	H Bond	Conventional H Bond
	A:ARG22	3.06606	H Bond	Conventional H Bond
	A:TYR99	3.01488	H Bond	Conventional H Bond
	A:TRP108	4.61561	Hy Bond	Pi-Alkyl
	A:HIS112	4.79727	Hy Bond	Pi-Alkyl
	A:HIS152	3.11406	HBond	Conventional H Bond
	A:HIS152	4.13512	Hy Bond	Pi-Alkyl
	A:ASP153	3.2513	Other	Pi-Anion
	A:HIS181	5.38791	Hy Bond	Pi-Alkyl
	A:ARG327	3.15163	H Bond	Conventional H Bond
6JBI vs. Camptothecin	B:VAL287	3.57577	H Bond	Carbon H Bond
	B:LYS294	2.91239	H Bond	Conventional H Bond
	B:VAL324	5.34311	Hy Bond	Pi-Alkyl
	B:LEU371	4.74267	Hy Bond	Alkyl
	B:ASN391	3.19834	H Bond	Conventional H Bond
	B:LEU392	3.16196	H Bond	Conventional H Bond
	B:LEU392	4.8772	Hy Bond	Alkyl
	B:VAL393	3.36434	H Bond	Conventional

				H Bond
6JBI vs. Rocaglaol	A:ARG22	4.67738	Hy Bond	Alkyl
	A:PRO24	4.62125	Hy Bond	Alkyl
	A:LEU44	4.28721	Hy Bond	Alkyl
	A:THR46	2.99097	H Bond	Conventional H Bond
	A:LEU48	4.95312	Hy Bond	Alkyl
	A:TYR99	3.6587	H Bond	Carbon H Bond
	A:TYR99	4.92019	Hy Bond	Pi-Alkyl
	A:TRP108	4.90005	Hy Bond	Pi-Alkyl
	A:HIS152	3.75287	Hy Bond	Pi-Pi Stacked
	A:ASP153	3.68267	H Bond	Carbon HBond
	A:ASP153	4.60817	Other	Pi-Anion
	A:HIS155	3.31986	H Bond	Conventional H Bond
	A:HIS155	5.01862	Hy Bond	Pi-Pi Stacked
	A:HIS181	5.12842	Hy Bond	Pi-Pi Stacked
5E9G vs. Pannellin	A:ASP118	4.73743	Other	Pi-Anion
	A:ASN134	3.66467	H Bond	Carbon H Bond
	A:LYS135	3.09262	H Bond	Conventional H Bond
	B:LYS135	2.87842	H Bond	Conventional H Bond
	A:LYS135	4.5186	Hy Bond	Alkyl
	A:HIS138	4.53618	Hy Bond	Pi-Alkyl

H= Hydrogen, Hy= Hydrophobic

Declarations

Ethical approval

Not applicable.

Funding

This study received no financial support.

Conflicts of interests

The authors declare no competing interests.

Data availability

The sequence data reported in this article are available in the FungiDB database (https://fungidb.org/fungidb/app/record/dataset/DS) and Protein Data Bank (https://www.rcsb.org/).

Acknowledgements

The authors would like to thank those who provided us the samples.

Supplementary information

Supplementary information supporting the results of the study are available in this article as Table S1 and S2.

Authors' contributions

M.A.K. and T. I. conceived and designed the study. M.A.K., M.A.A.M.K., J.M.S. and A.A. executed the bioinformatics analysis, interpreted the results and drafted the manuscript. D.R.G., M.N.H. and T.I. contributed intellectually to the interpretation and presentation of the results. Finally, all authors have approved the manuscript for submission.

References

1. Zhang, H., Zheng, X. & Zhang, Z. The Magnaporthe grisea species complex and plant pathogenesis. Molecular Plant Pathology **17**, 796 (2016).
2. Cruz, C. D. & Valent, B. Wheat blast disease: danger on the move. Tropical Plant Pathology **42**, 210–222 (2017).
3. Fernandez, J. & Orth, K. Rise of a cereal killer: the biology of Magnaporthe oryzae biotrophic growth. Trends in microbiology **26**, 582–597 (2018).
4. Singh, P. K. *et al.* Wheat blast: a disease spreading by intercontinental jumps and its management strategies. Frontiers in Plant Science, 1467 (2021).
5. Islam, M. T. *et al.* Emergence of wheat blast in Bangladesh was caused by a South American lineage of Magnaporthe oryzae. BMC biology **14**, 1–11 (2016).
6. Islam, M. T., Kim, K.-H. & Choi, J. Wheat blast in Bangladesh: the current situation and future impacts. The plant pathology journal **35**, 1 (2019).
7. Tembo, B. *et al.* Detection and characterization of fungus (Magnaporthe oryzae pathotype Triticum) causing wheat blast disease on rain-fed grown wheat (Triticum aestivum L.) in Zambia. PloS one **15**, e0238724 (2020).
8. Maciel, J. L. N. *et al.* Population structure and pathotype diversity of the wheat blast pathogen Magnaporthe oryzae 25 years after its emergence in Brazil. Phytopathology **104**, 95–107 (2014).
9. Duveiller, E., He, X. & Singh, P. K. Wheat blast: An emerging disease in South America potentially threatening wheat production. World wheat book **3**, 1107–1122 (2016).
10. Gladieux, P. *et al.* Gene flow between divergent cereal-and grass-specific lineages of the rice blast fungus Magnaporthe oryzae. MBio **9**, e01219-01217 (2018).
11. Kato, H. *et al.* Pathogenicity, mating ability and DNA restriction fragment length polymorphisms of Pyricularia populations isolated from Gramineae, Bambusideae and Zingiberaceae plants. Journal of General Plant Pathology **66**, 30–47 (2000).

12. Tosa, Y. *et al.* Genetic constitution and pathogenicity of Lolium isolates of Magnaporthe oryzae in comparison with host species-specific pathotypes of the blast fungus. Phytopathology **94**, 454–462 (2004).
13. Choi, J. *et al.* Comparative analysis of pathogenicity and phylogenetic relationship in Magnaporthe grisea species complex. PloS one **8**, e57196 (2013).
14. Roy, K. K. *et al.* First report of triticale blast caused by the fungus Magnaporthe oryzae pathotype Triticum in Bangladesh. Canadian Journal of Plant Pathology **43**, 288–295 (2021).
15. Roy, K. K. *et al.* First report of barley blast caused by Magnaporthe oryzae pathotype Triticum (MoT) in Bangladesh. Journal of General Plant Pathology **87**, 184–191 (2021).
16. Kimura, N. & Fukuchi, A. Management of melanin biosynthesis dehydratase inhibitor (MBI-D)-resistance in pyricularia oryzae using a non-MBI-D fungicidal application program for nursery boxes and a diclocymet and ferimzone mixture for field foliar applications. Journal of Pesticide Science **43**, 287–292 (2018).
17. Castroagudín, V. L. *et al.* Resistance to QoI fungicides is widespread in Brazilian populations of the wheat blast pathogen Magnaporthe oryzae. Phytopathology **105**, 284–294 (2015).
18. Srivastava, D. *et al.* Current status of conventional and molecular interventions for blast resistance in rice. Rice Science **24**, 299–321 (2017).
19. Chakraborty, M. *et al.* Inhibitory effects of linear lipopeptides from a marine Bacillus subtilis on the wheat blast fungus Magnaporthe oryzae Triticum. Frontiers in microbiology, 665 (2020).
20. Chakraborty, M., Mahmud, N. U., Ullah, C., Rahman, M. & Islam, T. Biological and biorational management of blast diseases in cereals caused by Magnaporthe oryzae. Critical Reviews in Biotechnology **41**, 994–1022 (2021).
21. Zhou, H. *et al.* Efficacy of Bacillus tequilensis strain JN-369 to biocontrol of rice blast and enhance rice growth. Biological Control **160**, 104652 (2021).
22. Kihara, J., Moriwaki, A., Ito, M., Arase, S. & Honda, Y. Expression of THR1, a 1, 3, 8-trihydroxynaphthalene reductase gene involved in melanin biosynthesis in the phytopathogenic fungus Bipolaris oryzae, is enhanced by near-ultraviolet radiation. Pigment cell research **17**, 15–23 (2004).
23. Jordan, D. B. *et al.* Structure-based design of inhibitors of the rice blast fungal enzyme trihydroxynaphthalene reductase. Journal of Molecular Graphics and Modelling **19**, 434–447 (2001).
24. Wilson, R. A. & Talbot, N. J. Under pressure: investigating the biology of plant infection by Magnaporthe oryzae. Nature Reviews Microbiology **7**, 185–195 (2009).
25. Wilson, R. A. *et al.* Tps1 regulates the pentose phosphate pathway, nitrogen metabolism and fungal virulence. The EMBO journal **26**, 3673–3685 (2007).
26. Fernandez, J. & Wilson, R. A. The sugar sensor, trehalose-6-phosphate synthase (Tps1), regulates primary and secondary metabolism during infection by the rice blast fungus: Will Magnaporthe oryzae's “sweet tooth” become its “Achilles’ heel”? *Mycology* **2**, 46–53 (2011).
27. Badaruddin, M. *et al.* Glycogen metabolic genes are involved in trehalose-6-phosphate synthase-mediated regulation of pathogenicity by the rice blast fungus Magnaporthe oryzae. PLoS pathogens **9**, e1003604 (2013).

28. Wang, Z. Y., Thornton, C. R., Kershaw, M. J., Debao, L. & Talbot, N. J. The glyoxylate cycle is required for temporal regulation of virulence by the plant pathogenic fungus Magnaporthe grisea. Molecular microbiology **47**, 1601–1612 (2003).
29. Lee, H.-S. *et al.* Inhibition of the pathogenicity of Magnaporthe grisea by bromophenols, isocitrate lyase inhibitors, from the red alga Odonthalia corymbifera. Journal of agricultural and food chemistry **55**, 6923–6928 (2007).
30. Udatha, D., Sugaya, N., Olsson, L. & Panagiotou, G. How well do the substrates KISS the enzyme? Molecular docking program selection for feruloyl esterases. Scientific reports **2**, 1–8 (2012).
31. Forli, S. *et al.* Computational protein–ligand docking and virtual drug screening with the AutoDock suite. Nature protocols **11**, 905–919 (2016).
32. Gilson, M. K. & Zhou, H.-X. Calculation of protein-ligand binding affinities. Annual review of biophysics and biomolecular structure **36**, 21–42 (2007).
33. Linn, C., Roy, S., Samant, L. & Chowdhary, A. Research Article In silico pharmacokinetics analysis and ADMET of phytochemicals of Datura. J. Chem. Pharm. Res **7**, 385–388 (2015).
34. Perpetua, N. S., Kubo, Y., Yasuda, N., Takano, Y. & Furusawa, I. Cloning and characterization of a melanin biosynthetic THR1 reductase gene essential for appressorial penetration of Colletotrichum lagenarium. Molecular plant-microbe interactions: MPMI **9**, 323–329 (1996).
35. Wawrzak, Z. *et al.* High-resolution structures of scytalone dehydratase-inhibitor complexes crystallized at physiological pH. Proteins: Structure, Function, and Bioinformatics **35**, 425–439 (1999).
36. Thompson, J. E. *et al.* The second Naphthol reductase of fungal melanin biosynthesis inMagnaporthe grisea: Tetrahydroxynaphthalene reductase. Journal of Biological Chemistry **275**, 34867–34872 (2000).
37. Yamada, N. *et al.* Enzymatic characterization of scytalone dehydratase Val75Met variant found in melanin biosynthesis dehydratase inhibitor (MBI-D) resistant strains of the rice blast fungus. Bioscience, biotechnology, and biochemistry **68**, 615–621 (2004).
38. Song, X.-S. *et al.* Trehalose 6-phosphate phosphatase is required for development, virulence and mycotoxin biosynthesis apart from trehalose biosynthesis in Fusarium graminearum. Fungal Genetics and Biology **63**, 24–41 (2014).
39. Zou, Y. *et al.* PstTPS1, the trehalose-6-phosphate synthase gene of Puccinia striiformis f. sp. tritici, involves in cold stress response and hyphae development. Physiological and Molecular Plant Pathology **100**, 201–208 (2017).
40. Liu, N., Tu, J., Dong, G., Wang, Y. & Sheng, C. Emerging new targets for the treatment of resistant fungal infections. Journal of medicinal chemistry **61**, 5484–5511 (2018).
41. García, M. D. & Argüelles, J. C. Trehalase inhibition by validamycin A may be a promising target to design new fungicides and insecticides. Pest Management Science **77**, 3832–3835 (2021).
42. Dunn, M., Ramirez-Trujillo, J. & Hernández-Lucas, I. Major roles of isocitrate lyase and malate synthase in bacterial and fungal pathogenesis. Microbiology **155**, 3166–3175 (2009).
43. Shin, D.-S., Lee, T.-H., Lee, H.-S., Shin, J. & Oh, K.-B. Inhibition of infection of the rice blast fungus by halisulfate 1, an isocitrate lyase inhibitor. FEMS microbiology letters **272**, 43–47 (2007).

44. Joshi, T., Joshi, T., Sharma, P., Pundir, H. & Chandra, S. In silico identification of natural fungicide from Melia azedarach against isocitrate lyase of Fusarium graminearum. Journal of Biomolecular Structure and Dynamics **39**, 4816–4834 (2021).
45. Jorgensen, W. L. & Tirado–Rives, J. Molecular modeling of organic and biomolecular systems using BOSS and MCPRO. Journal of Computational Chemistry **26**, 1689–1700 (2005).
46. Al-Shabib, N. A. *et al.* Molecular insight into binding behavior of polyphenol (rutin) with beta lactoglobulin: Spectroscopic, molecular docking and MD simulation studies. Journal of Molecular Liquids **269**, 511–520 (2018).
47. Leeson, P. Chemical beauty contest. Nature **481**, 455–456 (2012).
48. Refsgaard, H. H. *et al.* In silico prediction of membrane permeability from calculated molecular parameters. Journal of medicinal chemistry **48**, 805–811 (2005).
49. Chang, L. C. *et al.* 2, 4, 6-Trisubstituted pyrimidines as a new class of selective adenosine A1 receptor antagonists. Journal of medicinal chemistry **47**, 6529–6540 (2004).
50. Steinberg, G. *et al.* A lipophilic cation protects crops against fungal pathogens by multiple modes of action. Nature communications **11**, 1–19 (2020).
51. Mullard, A. Re-assessing the rule of 5, two decades on. Nature reviews. Drug discovery **17**, 777 (2018).
52. Veber, D. F. *et al.* Molecular properties that influence the oral bioavailability of drug candidates. Journal of medicinal chemistry **45**, 2615–2623 (2002).
53. Xu, S. *et al.* Effects of camptothecin on the rice blast fungus Magnaporthe oryzae. Pesticide biochemistry and physiology **163**, 108–116 (2020).
54. Oikawa, H. Biosynthesis of structurally unique fungal metabolite GKK1032A2: indication of novel carbocyclic formation mechanism in polyketide biosynthesis. The Journal of Organic Chemistry **68**, 3552–3557 (2003).
55. Nguyen, Q. T. *et al.* Antifungal activity of a novel compound purified from the culture filtrate of Biscogniauxia sp. O821 against the rice blast fungus Magnaporthe oryzae. Journal of General Plant Pathology **84**, 142–147 (2018).
56. Engelmeier, D., Hadacek, F., Pacher, T., Vajrodaya, S. & Greger, H. Cyclopenta [b] benzofurans from Aglaia species with pronounced antifungal activity against rice blast fungus (Pyricularia grisea). Journal of Agricultural and Food Chemistry **48**, 1400–1404 (2000).
57. Lucas, J. A., Hawkins, N. J. & Fraaije, B. A. The evolution of fungicide resistance. Advances in applied microbiology **90**, 29–92 (2015).
58. Hawkins, N. & Fraaije, B. Fitness penalties in the evolution of fungicide resistance. Annual Review of Phytopathology **56**, 339–360 (2018).
59. Berman, H. M. *et al.* The protein data bank. Acta Crystallographica Section D: Biological Crystallography **58**, 899–907 (2002).
60. Sharma, S., Sharma, A. & Gupta, U. Molecular Docking studies on the Anti-fungal activity of Allium sativum (Garlic) against Mucormycosis (black fungus) by BIOVIA discovery studio visualizer 21.1. 0.0. Annals of Antivirals and Antiretrovirals **5**, 028–032 (2021).

61. Masand, V. H. & Rastija, V. PyDescriptor: A new PyMOL plugin for calculating thousands of easily understandable molecular descriptors. Chemometrics and Intelligent Laboratory Systems **169**, 12–18 (2017).
62. Cheng, T., Pan, Y., Hao, M., Wang, Y. & Bryant, S. H. PubChem applications in drug discovery: a bibliometric analysis. Drug discovery today **19**, 1751–1756 (2014).
63. Oellien, F. & Nicklaus, M. Online SMILES translator and structure file generator. National Cancer Institute **29**, 97–101 (2004).
64. Ahammad, F. *et al.* Pharmacoinformatics and molecular dynamics simulation-based phytochemical screening of neem plant (Azadiractha indica) against human cancer by targeting MCM7 protein. Briefings in Bioinformatics **22**, bbab098 (2021).
65. Mohammad, T., Mathur, Y. & Hassan, M. I. InstaDock: A single-click graphical user interface for molecular docking-based virtual high-throughput screening. Briefings in Bioinformatics **22**, bbaa279 (2021).
66. Yuliana, D., Bahtiar, F. I. & Najib, A. In silico screening of chemical compounds from roselle (Hibiscus Sabdariffa) as angiotensin-I converting enzyme inhibitor used PyRx program. ARPN J. Sci. Technol **3**, 1158–1160 (2013).
67. Kumar, N., Mishra, S. S., Sharma, C. S., Singh, H. P. & Singh, H. In silico pharmacokinetic, bioactivity and toxicity evaluation of some selected anti-ulcer agents. Int J Pharm Sci Res **9**, 68–71 (2017).
68. Bittencourt, J. A. *et al.* In silico evaluation of ibuprofen and two benzoylpropionic acid derivatives with potential anti-inflammatory activity. Molecules **24**, 1476 (2019).

Figures

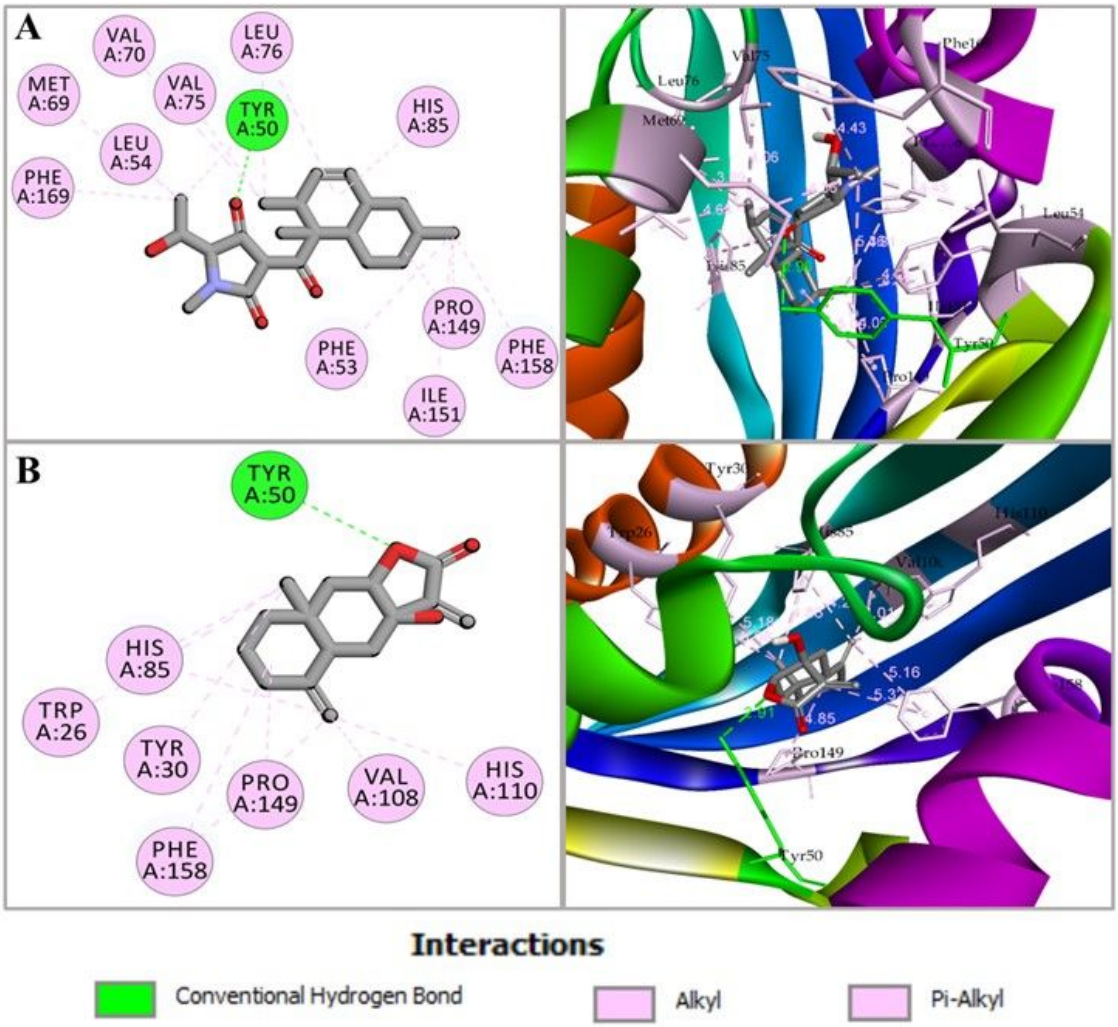

Figure 1

(A) Cryptocin docked in complex with Scytalone dehydratase (PDB ID: 1STD); forming a hydrogen bond with side chain A:TYR50, whereas hydrophobic interactions with residues A:LEU76, A:PRO149, A:ILE151, A:VAL70, A:VAL75, A:LEU54, A:MET69, A:TYR50, A:PHE53, A:HIS85, A:PHE158, A:PHE169**. (B)** Interaction between compound HDFO and Scytalone dehydratase illustrated. 2D interaction analysis shown at left and 3D interaction analysis shown at right side.

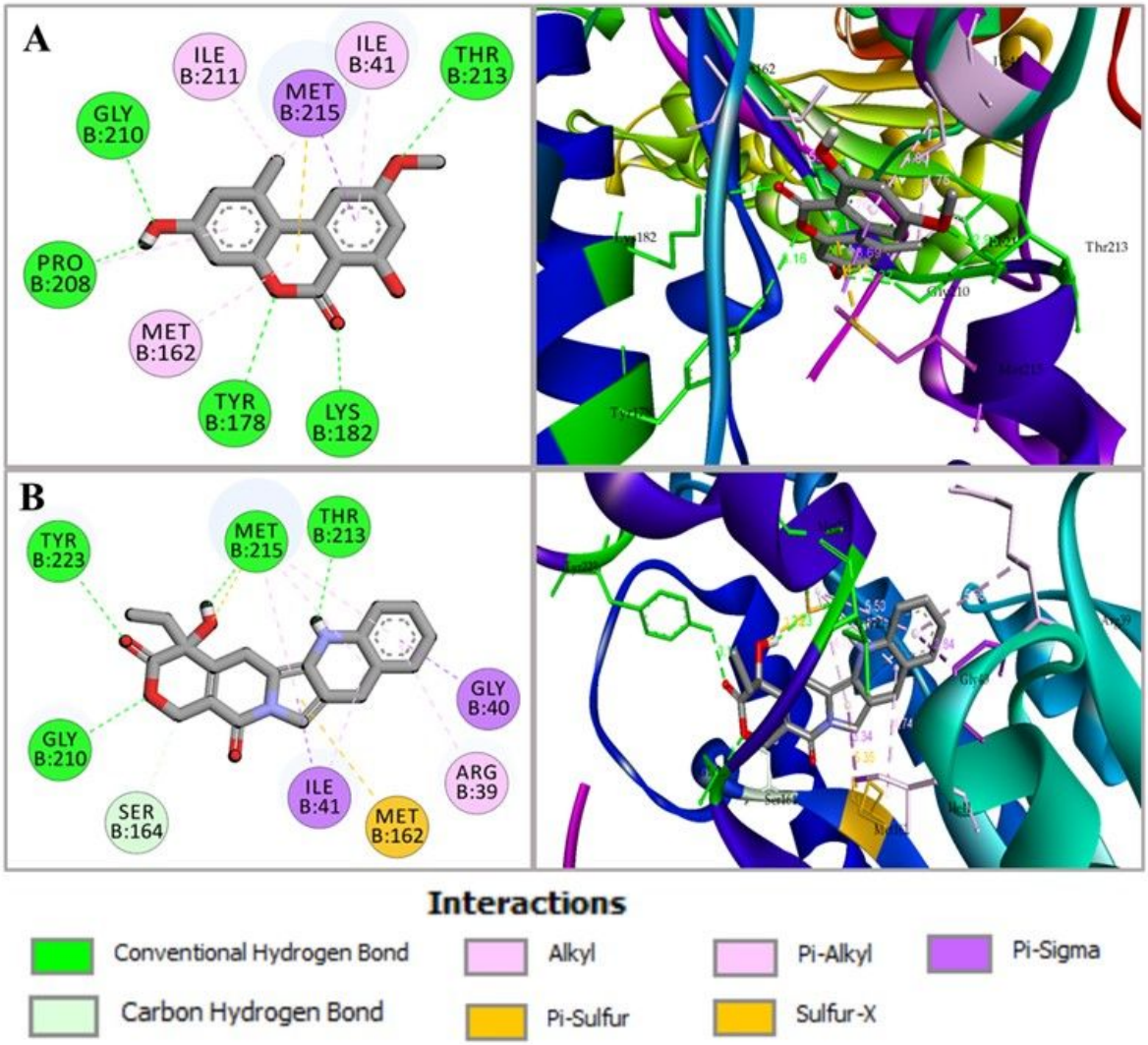

Figure 2

(A) Interaction between Trihydroxynaphthalene reductase and compound Alternariol-monomethyl-ether illustrated. **(B)** Camptothecin docked in complex with Trihydroxynaphthalene reductase (PDB ID: 1YBV); Camptothecin showed hydrogen bond with residues B:GLY210, B:TYR223, B:MET215, B:THR213, and B:SER164 hydrophobic non bonded interactions are formed with B:GLY40, B:ILE41, B:MET215 and B:ARG39 and other bonds are B:MET215 and B:MET162. 2D interaction analysis shown at left and 3D interaction analysis shown at right side.

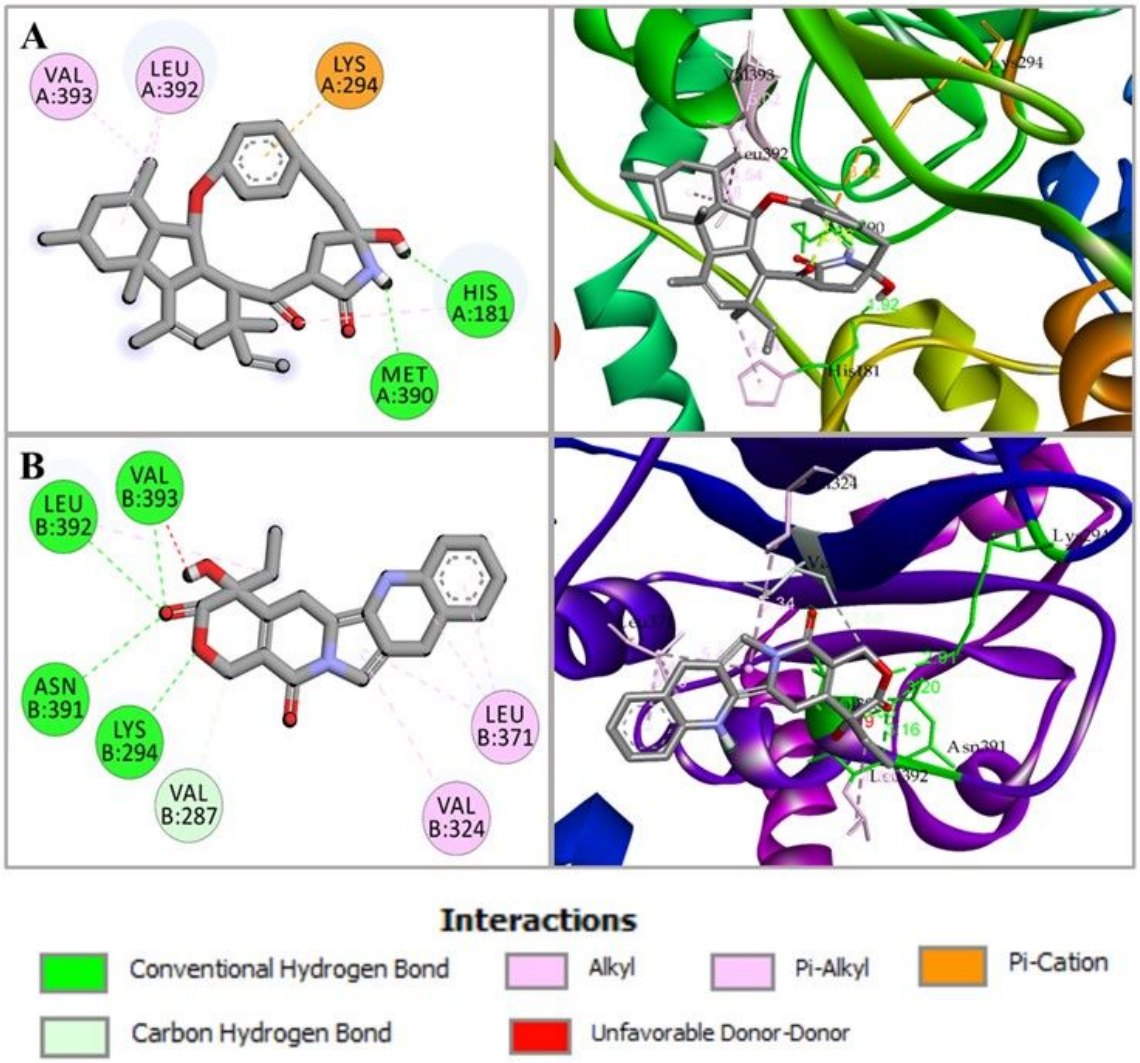

Figure 3

(A) GKK1032A2 Docked in complex with trehalose-6-phosphate synthase 1 or Tps1 (PDB ID: 6JBI); Hydrogen bonds favor the docking interactions of GKK1032A2 with A:MET390, A:HIS181, and A:LYS294, while non-bonded hydrophobic interactions are favored by A:LEU392, A:VAL393, and A:HIS181. **(B)** Interaction between trehalose-6-phosphate synthase 1 or Tps1 and compound Camptothecin illustrated. 2D interaction analysis shown at left and 3D interaction analysis shown at right side.

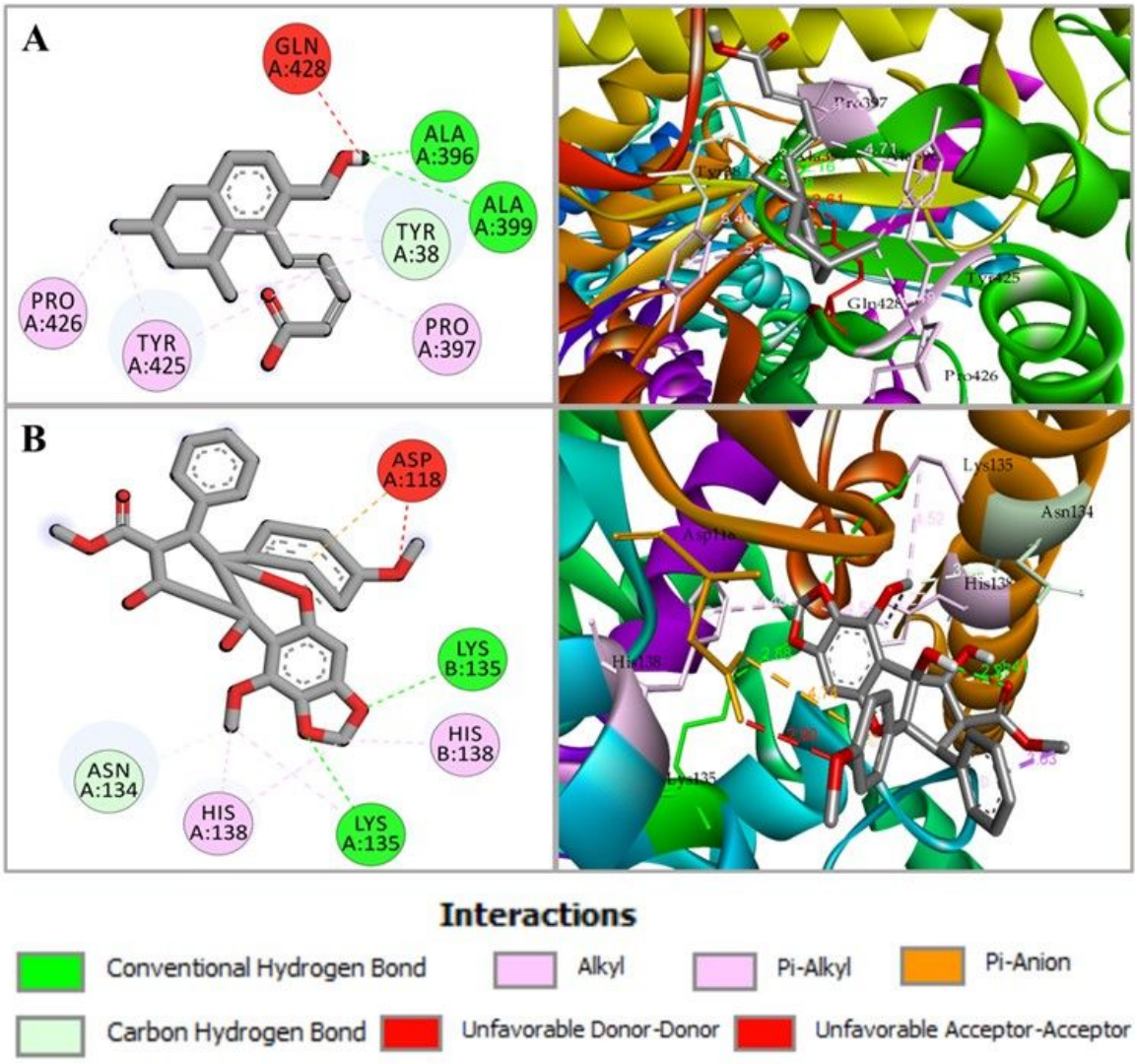

Figure 4

(A) Arohynapene-B docked in complex with isocitrate lyase enzyme (PDB ID: 5E9G); The binding conformations were analyzed, and we identified that arohynapene-B formed a hydrogen bond with A:ALA396, A:ALA399 and A:TYR38. In addition, several residues A:PRO397, A:PRO426, A:TYR38, A:TYR425 formed hydrophobic interactions. (B) Pannellin formed hydrogen bond with A:LYS135, B:LYS135 and A:ASN134 and hydrophobic interactions with residues A:LYS135 and A:HIS138 whereas electrostatic interaction with A:ASP118. 2D interaction analysis shown at left and 3D interaction analysis shown at right side.

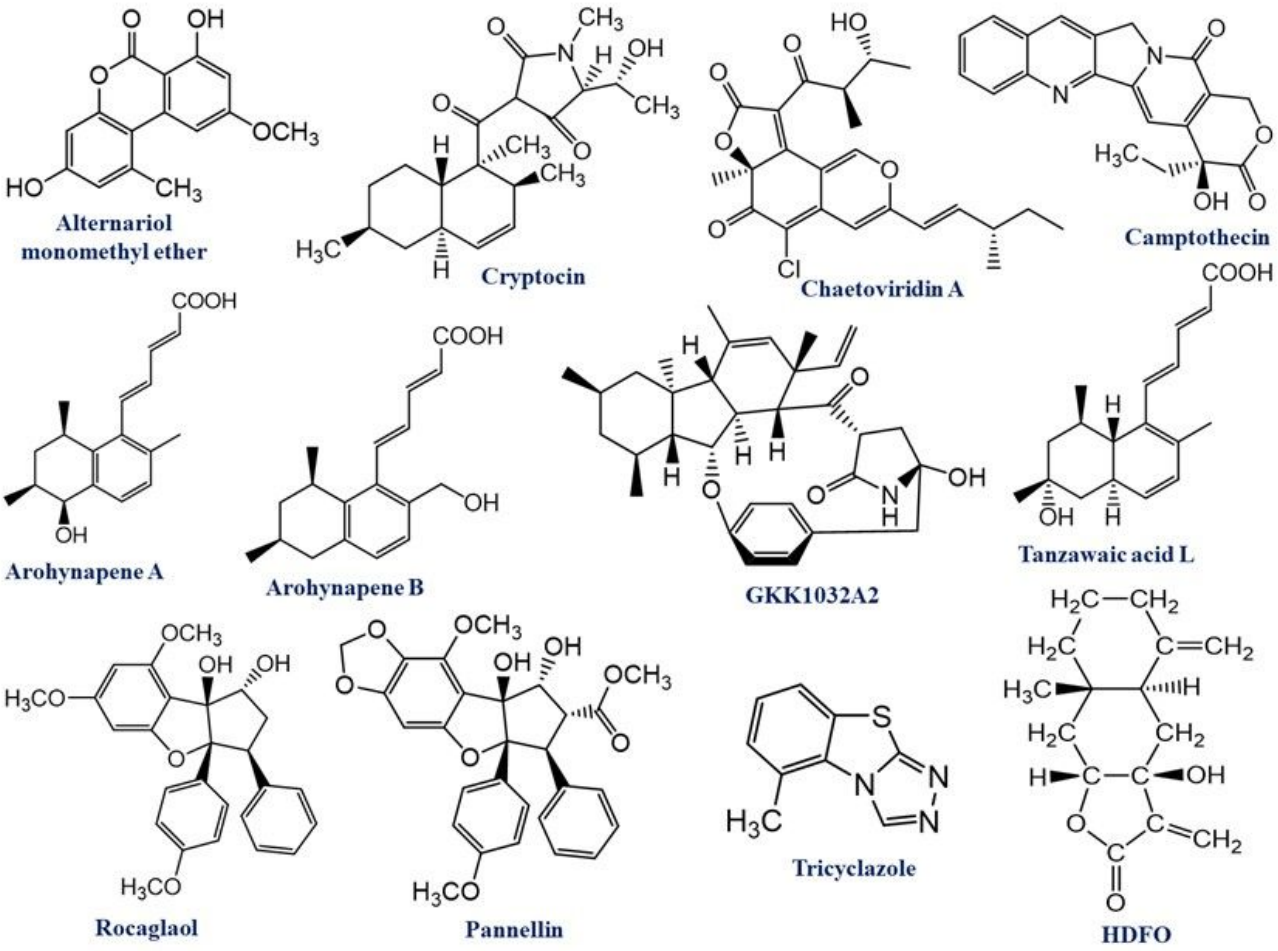

Figure 5

Two-dimentional (2D) chemical structure of the 12 top ranked selected compounds.